say the top 10 m, because the groundwater salinity below this depth does not change over short periods. It does change, however, when deep tubewells are installed and operated. When there is deep pumping, therefore, the assessment must include data from a much greater depth to take into account the effects of partial penetration by the tubewells.

To estimate the changes in the salt concentration of the groundwater reservoir, it is necessary to make a water and salt balance of the unsaturated zone. It is through this zone that water and salt move to the groundwater. In areas with shallow watertables, water and salt move to the surface through capillary rise, where the water evaporates and the salt concentrates in the upper soil layers.

If we have a salt balance of the unsaturated zone, we can estimate the net quantity of salt that enters the groundwater reservoir through the percolation of precipitation and irrigation water. The salt balance of the groundwater reservoir can then be assessed with this quantity (Brown et al. 1977).

For salt balance studies, we can use the same data we used for the total water balance, the water balance of the unsaturated zone, and the water balance of the groundwater reservoir. These studies are usually made in experimental plots or key plots, in combination with studies of soil water and groundwater movements. A network of nested piezometers is necessary to measure the water levels and to take water samples for tests of the salt concentration. It is common to measure the salt concentrations in the unsaturated zone before and after the soil is leached and before and after the growing season (Chapter 15).

## 16.3 Numerical Groundwater Models

### 16.3.1 General

The process of setting up partial or integrated water balances can be complicated and time-consuming. Spatial variation in the contributing components can make it necessary to split up the study area into various sub-areas. Each of the sub-areas will require a separate water balance, and all of these balances will have to be aggregated. In addition, the sub-areas may require a monthly water balance, and these will also have to be aggregated if a seasonal or annual water balance is needed.

Another complicating factor is that groundwater exhibits a number of non-linear features. These include the hydraulic conductivity and specific yield of the aquifer system (which are functions of the watertable height), moving boundaries, and the effect of hysteresis on the relationship between capillary flux and soil water content.

Problems of non-linearity and spatial variation are quite often oversimplified or even neglected when water balances are being set up manually. To avoid the risk of oversimplification, it is possible to use numerical groundwater models to solve the problems. A groundwater model can be defined as a simplified version of the real groundwater system. It describes the flow characteristics and gives pertinent assumptions and constraints. It expresses the conceptual representation of the system in causal relationships among the system's various components and between the system and its environment.

Groundwater models are based on two well-known equations: Darcy's equation and the equation of conservation of mass (Chapter 7). The combination of these two equations results in a partial differential equation that can be solved by numeric approximation. The two best-known approximation methods are the finite difference method and the finite element method. Both require that space be divided into small but finite intervals. The sub-areas thus formed are called nodal areas, as they each have a node that connects it mathematically to its neighbours. The nodal areas make it possible to replace the partial differential equation with a set of algebraic equations.

### 16.3.2 Types of Models

There are many types of groundwater models, but for our purposes let us start with a description of steady-state and unsteady-state models. As their name suggests, steady-state models assume that groundwater flow is in steady state, i.e. that the hydraulic heads do not change with time, and that the change in storage is equal to zero. Steady-state models are often used in situations where the hydrologic conditions are either average or do not change much over time. Unsteady-state models assume that the hydraulic heads change with time. Although these models are better at simulating the actual behaviour of groundwater systems, they require far more input data than do steady-state models. Because these data are scarce, unsteady-state models are not used as often as steady-state models.

For both types of models, we must input the geometry of the aquifer system, the type of aquifer, and the hydraulic characteristics of the aquifer. Although there may be variation from one node to another, we can assume that within a nodal area these data are constant and time-independent.

For steady-state models, we must prescribe external stress at the internal nodes and boundary conditions at the boundary nodes. Examples of external stress are recharge of the groundwater system by infiltrating rainfall and discharge from the groundwater system by tubewell pumpage. As boundary conditions, we must prescribe either a constant head or a constant flux.

Time simulation in unsteady-state models is a succession of small but finite intervals. For each of these time steps, specific values for external stress must be prescribed at the internal nodes and values for head or flux at the boundary nodes, as they may change with time. Initial conditions must also be prescribed. Usually, we can interpolate the values of the head at the internal nodes from a watertable contour map.

Now that we have considered these models, let us look at prediction models. Prediction models simulate the behaviour of the groundwater system and its response to stress. They are categorized as either unsaturated-zone models, saturated-zone models, or integrated models.

Unsaturated-zone models simulate vertical, one-dimensional flow. They use a succession of different soil layers, usually extending from the land surface to the saturated zone, to represent a vertical soil column. To each of these soil layers, they attribute a soil-moisture retention curve and values of the hydraulic conductivity as a function of soil-moisture content. In addition, they require values for the initial moisture content in the profile and for the boundary conditions at the top and bottom of the column. The boundary conditions at the top are described by values of rainfall, potential soil evaporation, and potential evapotranspiration. The boundary conditions at the bottom are described by pressure head or flux conditions. The soil layers themselves may consist of various compartments. Each compartment is represented by a nodal point; the values for pressure head, unsaturated hydraulic conductivity, and soil moisture content are calculated at these points.

Saturated-zone models simulate the horizontal, two-dimensional flow. They discretize the aquifer system into a network of nodal areas. To each nodal area, they attribute values for the thickness, the saturated hydraulic conductivity, the specific yield, and the storage coefficient. In addition, they require values for the initial pressure heads in each nodal area and for the boundary conditions at the top and sides (lateral boundary conditions). We can obtain a value for the boundary conditions at the top by calculating the net recharge to the aquifer system first and then setting up water balances for the unsaturated zone. To define the lateral boundary conditions, we can use pressure head conditions and flux conditions, but it is more common to use pressure head conditions.

Each nodal area can consist of various aquifer types. The multi-layered (pseudo three-dimensional) groundwater models simulate the interaction between the various aquifers by calculating vertical flow through the aquitards. Each nodal area is represented by a nodal point, or by different nodal points in multi-layered aquifers; values for the hydraulic head are calculated at these points.

A third type of prediction model is the integrated model. These models can integrate the flow in the unsaturated zone with the flow at the land surface, with the flow in the saturated zone, with both of these flows, and with crop production.

All three types of models predict pressure head and groundwater head at the nodes as a function of prescribed, time-varied, external stress. They use these heads to calculate the relevant water balance components – net recharge, horizontal and vertical flow rates, changes in storage – for each nodal area. It is common to aggregate these components to obtain a water balance for the whole model area.

There is a special category of groundwater models that run in the so-called 'inverse mode'. These models calculate the external stress as a function of prescribed time-varied heads. They can be particularly useful for determining the drainable surplus from field investigations.

For more information on all these models, refer to Feddes et al. (1988), IGWMC (1992), and to Volp and Lambrechts (1988).

## 16.4 Examples of Water Balance Analysis

Let us now consider a rectangular farm, 1600 m long and 860 m wide, that is located in a flat alluvial plain. An irrigation channel crosses the farm approximately in the middle. The crops cultivated on the farm are irrigated with water from this canal. Rice is grown in a strip on both sides of the canal, and cereals and other field crops on the remaining parts of the farm.

The lands surrounding this farm are also cultivated, but because of a shortage of irrigation water, they are not supplied with water from the canal. Some farmers have a shallow hand-dug well and use its water to irrigate small patches of the land.

During the irrigation season, it was found that the watertable in parts of the irrigated farm was rather shallow, and the question arose whether the farm land needed artificial drainage.

Shallow piezometers were placed in a regular grid, and monthly readings were made of the depths to the watertable. This observation network was also surveyed, so the observed watertable depth data could be converted to absolute watertable elevation data. Groundwater samples were taken from the piezometers and their electrical conductivity was determined.

### 16.4.1 Processing and Interpretation of Basic Data

The above data were processed to produce depth-to-watertable maps, watertable contour maps, and electrical conductivity maps (Chapter 2). Their results and interpretation are briefly summarized below.

Figure 16.12 shows the depth-to-watertable map on a certain date in the irrigation season. The watertable in the middle of the farm is shallow, less than 1 m below the land surface, and along the canal, even less than 0.5 m. This is caused partly by leakage from the canal, but mainly by the heavy percolation from the rice fields near the canal. In the other parts of the farm, less irrigation water is applied (cereals and field crops), percolation is less, and the watertable deeper (2–3 m).

The direction of groundwater flow can be derived from the watertable contour map (Figure 16.13). The flow direction is perpendicular to the contour lines (equipotential lines). In the middle of the farm, near the canal, a groundwater mound has formed from where water flows in all directions. Everywhere along the farm boundaries groundwater flows out from the farm, except in the northeast and southeast where the boundary is nearly perpendicular to the watertable contour lines. This means that these parts of the boundary are flow lines across which, by definition, no groundwater flows. Along the other parts of the farm boundary, the watertable gradient varies from about 1:200 to 1:400. This indicates that the aquifer system is more or less homogeneous.

Figure 16.14 shows the electrical conductivity map of the shallow groundwater. The least saline groundwater is found in the middle of the farm, even though the watertable there is at its shallowest. The heavy percolation in this part of the farm apparently prevents capillary rise, and since groundwater flows away from this area in all directions, soil and groundwater cannot become salinized. In the direction of flow, however, the salinity increases rapidly, and just beyond the farm boundaries, i.e. in the non-irrigated areas, it reaches its highest values (EC = 20 to 25 dS/m). Farmers in these areas suffer in three ways: they do not receive surface water from the canal for irrigation because it is in short supply, they cannot use groundwater because it has become too saline, and their lands are in danger of becoming salinized because the inflow of groundwater from the irrigated farm causes the watertable in their land to rise to or within critical heights and the capillary rise to become important.

From this information, it is clear that no artificial drainage for salinity control is required for the irrigated farm itself. Even for watertable control no drainage is required because rice is being grown in the area with the shallowest groundwater depths. To protect the surrounding area, it would, however, be advisable to impose certain watertable control measures within the irrigated farm. Changing the cropping

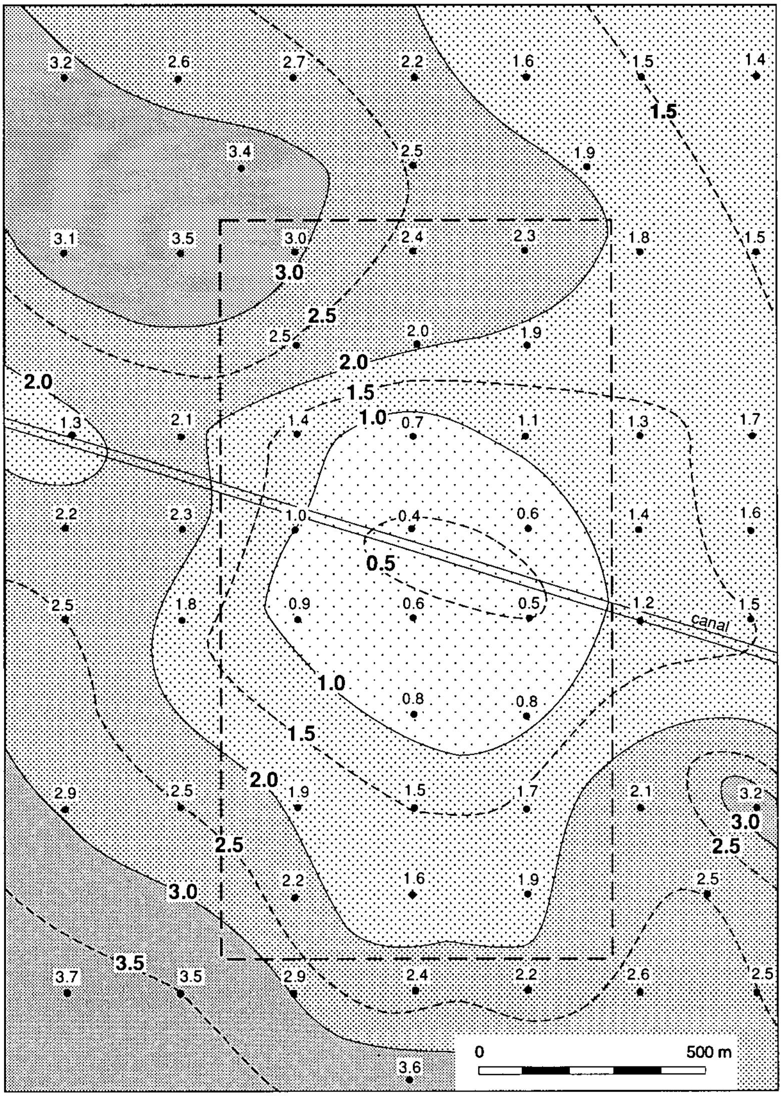


Figure 16.12 Depth-to-watertable map:
• 1.6 = observation well, watertable depth 1.6 m below soil surface

pattern (rice should never be cultivated on relatively light soils) will undoubtedly alleviate the problem.

### 16.4.2 Water Balance Analysis With Flow Nets

So far, we have discussed how to make a qualitative water balance analysis. Here, and in the next section, we shall discuss how to make a quantitative analysis by setting up water balances for the saturated zone.

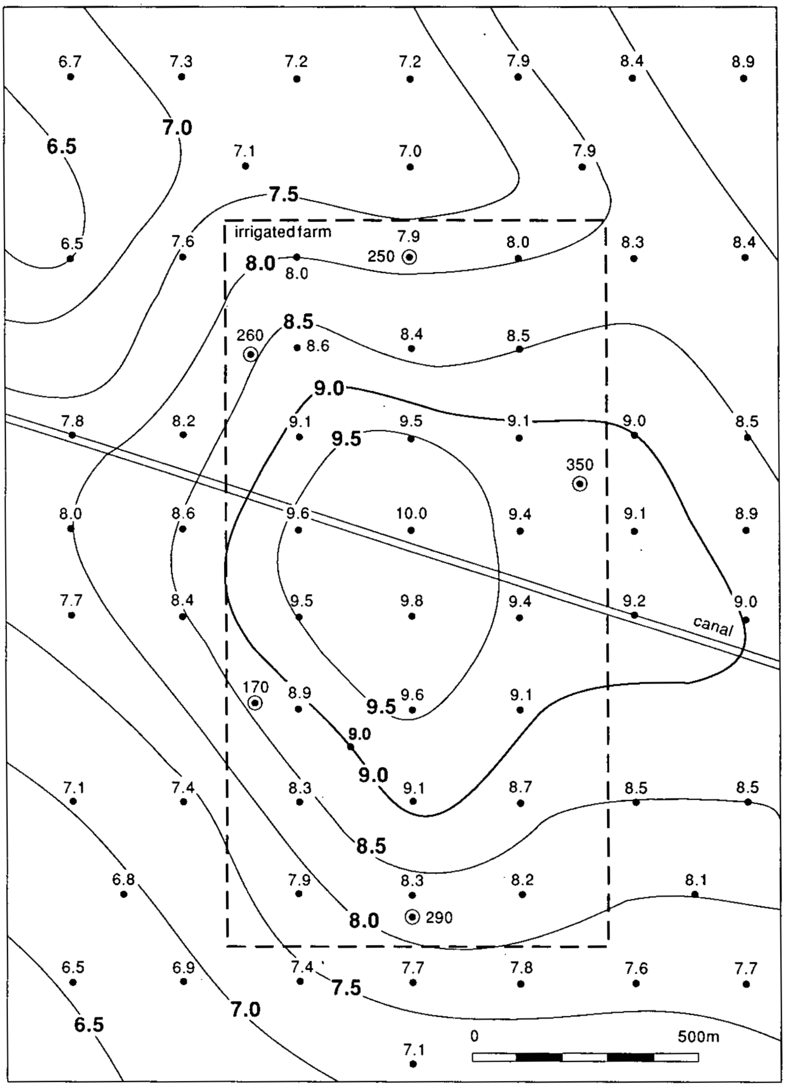


Figure 16.13 Watertable contour map:
• 8.3 = observation well, watertable elevation 8.3 m above sea level
⊙ 290 = aquifer test site, transmissivity KD = 290 $m^2/d$

*Example 16.1*
Let us make a water balance for the irrigated farm. For simplicity, let us assume that the data in Figures 16.12, 16.13, and 16.14 are representative of the irrigation season, i.e. let us assume that the groundwater system is in a steady state during the irrigation season.

To calculate the rate of groundwater flow across the farm boundaries, we need to know the watertable gradient and the aquifer transmissivity. Because the equipotential lines in Figure 16.13 do not coincide with the farm boundaries, but cross

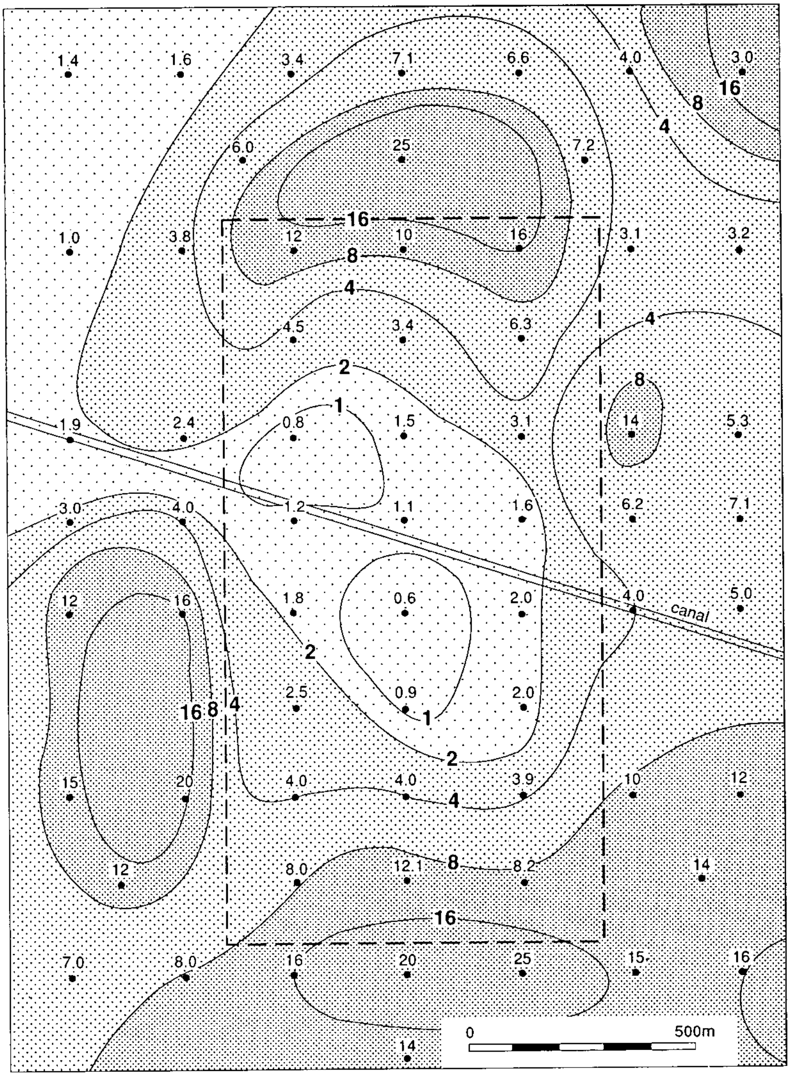


Figure 16.14 Electrical conductivity of the shallow groundwater in dS/m

them obliquely, we must construct a flow net (Figure 16.15). This should be done according to the following specifications:

- To construct the first 'square', select a pair of equipotential lines that run along both sides of the boundary of the water balance area. Draw a first flow line at an arbitrarily chosen location; the smoothly drawn flow line should intersect both equipotential lines at right angles. Draw a second flow line in such a manner that the distance between the two equipotential lines midway between the two flow lines is equal to the distance between the two flow lines midway between the two equipotential lines. Like this, a square will generally have four slightly curved sides;
- To construct the next square, use the same pair of equipotential lines if these lines

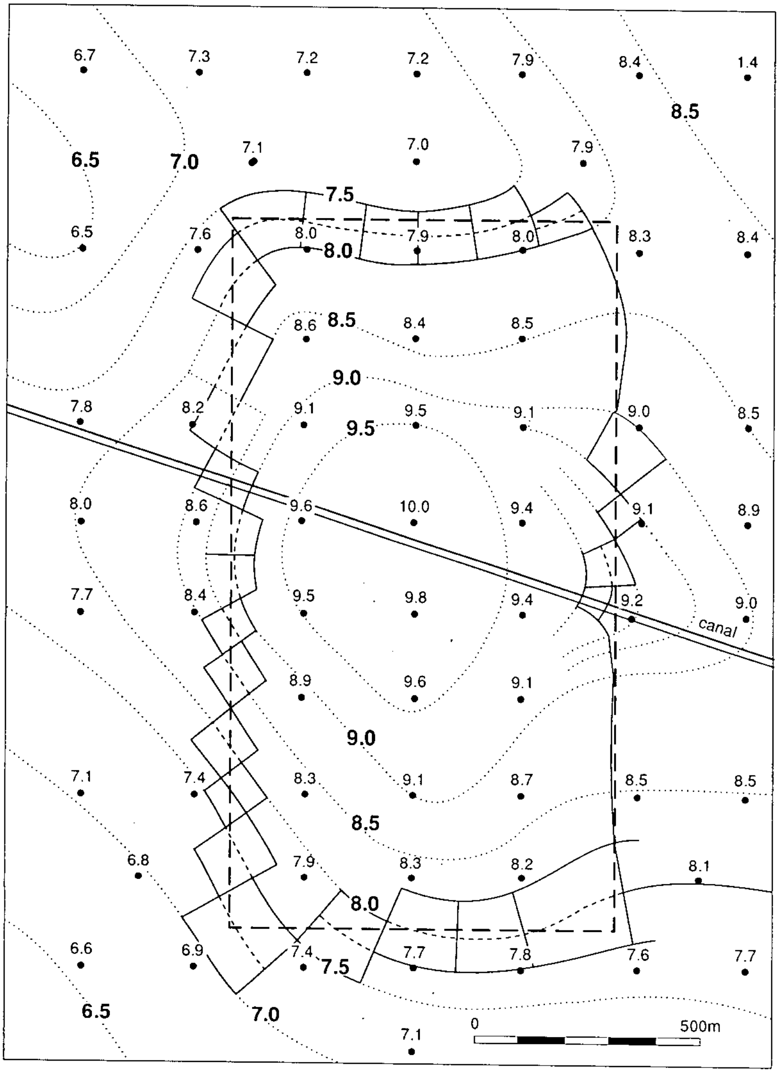


Figure 16.15 Watertable contour map with a flow net constructed along the farm boundaries

still follow the boundary of the water balance area. Draw the next flow line. If the equipotential lines start to deviate from the area boundary, extend the flow line to another pair of equipotential lines that do follow the boundary. The squares should follow the boundaries of the water balance area as closely as possible;

- Continue this process until the last flow line drawn coincides with the first flow line drawn, i.e. until the water balance area is fully enclosed by squares.

Figure 16.15 shows that to construct a system of squares along the four boundaries of the irrigated farm, it was necessary in some places to reduce the contour interval from 0.50 m to 0.25 m, and even to 0.10 m and 0.05 m in the east of the farm.

Information on the transmissivity of the aquifer was obtained from the analysis of five aquifer test sites. These sites are shown in Figure 16.13 together with their transmissivity values, which were attributed to certain sections of the farm boundary.

We can calculate the rate of horizontal groundwater flow through each square using Darcy's equation

$$Q = KD\,s\,\Delta y = KD\frac{\Delta h}{\Delta x}\Delta y \qquad (16.13)$$

with

| | | |
|---|---|---|
| KD | = | the transmissivity of the aquifer ($m^2/d$) |
| s | = | the hydraulic gradient (–) |
| $\Delta y$ | = | the width over which groundwater flow occurs, i.e. the perpendicular distance between two flow lines (m) |
| $\Delta h$ | = | the difference in hydraulic head between two contour lines (m) |
| $\Delta x$ | = | the distance between two contour lines, as measured in the direction of flow (m) |

Because the squares were constructed so that $\Delta x$ equals $\Delta y$, the total groundwater flow across the boundaries of the water balance area reduces to $Q = n\,KD\,\Delta h$, where n is the number of squares provided the proper KD and $\Delta h$ values are attributed to each square.

For the flow net in Figure 16.15, this procedure yielded the following results: starting in the northeast and moving anti-clockwise

$$\begin{aligned} Q = {} & (1 \times 250 \times 0.25) + (5 \times 250 \times 0.50) + (3 \times 260 \times 0.50) + \\ & (7 \times 170 \times 0.50) + (6 \times 290 \times 0.50) + (1 \times 350 \times 0.05) + \\ & (3 \times 350 \times 0.10) = 2665\ m^3/d \end{aligned}$$

For the irrigated farm, Equation 16.5 (the groundwater balance) reduces to

$$R - G - 1000\frac{Q_{go}}{A} = 0 \qquad (16.14)$$

in which $Q_{go}$ is the horizontal outflow of groundwater. This is so because:

- We assumed the aquifer could be treated as an unconfined aquifer (no vertical inflow or outflow of groundwater);
- We observed no horizontal groundwater inflow anywhere along the boundaries of the irrigated farm, so $Q_{gi} = 0$;
- We assumed the groundwater system was in a steady state during the irrigation season, so $\mu\,\Delta h/\Delta t = 0$.

If we assume that $Q_{go} = 2665\ m^3/d$ and that $A = 1600 \times 860 = 1\,376\,000\ m^2$, then Equation 16.14 yields

$$R - G = 1000\frac{2665}{1\,376\,000} = 1.9\ mm/d$$

And if we assume that steady-state conditions prevail in the unsaturated zone, Equation 16.4 then yields $I - E = 1.9$ mm/d. This is the net infiltration rate, and it represents an average taken over the total area of the irrigated farm. We can expect the net recharge to be substantially higher in the middle of the farm and lower along the fringes.

### 16.4.3 Water Balance Analysis With Models

So far, we have used the groundwater balance to estimate the natural drainage (some 2 mm/d) on the irrigated farm. This value does not, however, represent the drainable surplus, as we shall see below.

*Example 16.2*
Let us now use a groundwater simulation model for the saturated zone to get additional information on the irrigated farm's drainable surplus. To develop the model, we can use an updated version of the SGMP groundwater model (Boonstra and De Ridder 1990). The water balance area on the farm is discretized into a network of rectangles, called a 'nodal network' (Figure 16.16). Most of the nodes coincide with the locations of the observation wells shown in Figure 16.12. Because the network of observation wells is slightly irregular, it is necessary to use the watertable contour map to interpolate the watertable elevation for the nodes that did not coincide with observation wells.

The observed (interpolated) watertable elevations were assigned to the nodes of the groundwater model. The reported transmissivity values from the five aquifer test sites were used to make a map that showed lines of equal transmissivity. The nodal network map was superimposed on the transmissivity map and, for each nodal area, the corresponding transmissivity value was determined and fed into the database of the model. The model was then run in the inverse mode.

The model yielded a set of nodal net recharges (Figure 16.16). The recharge values range from 9.6 mm/d in the middle of the farm to – 5.6 mm/d in certain areas. In these other areas, the percolation losses from irrigation are apparently so small that the capillary rise rate exceeds them. The first line in Table 16.3 shows the overall water balance of the irrigated farm according to the inverse model run. Note that the boundaries of the farm do not coincide exactly with the sides of the nodal areas.

Table 16.3 shows that the total groundwater outflow calculated from the flow net corresponds reasonably well with the outflow calculated by the model. The similarity proves that a groundwater model run in inverse mode will yield the spatial distribution of net recharge values. In addition, it proves that the model can simulate a watertable

Table 16.3 Water balance components of the irrigated farm according to the model runs, in $m^3/d$

| Actual and simulated watertable elevations | Net recharge | Groundwater outflow | Drain discharge |
|---|---|---|---|
| Actual situation | 2551 | 2551 | - |
| Watertable depth ≥ 1.0 m | 2551 | 2033 | 518 |
| Watertable depth ≥ 1.5 m | 2551 | 1377 | 1174 |

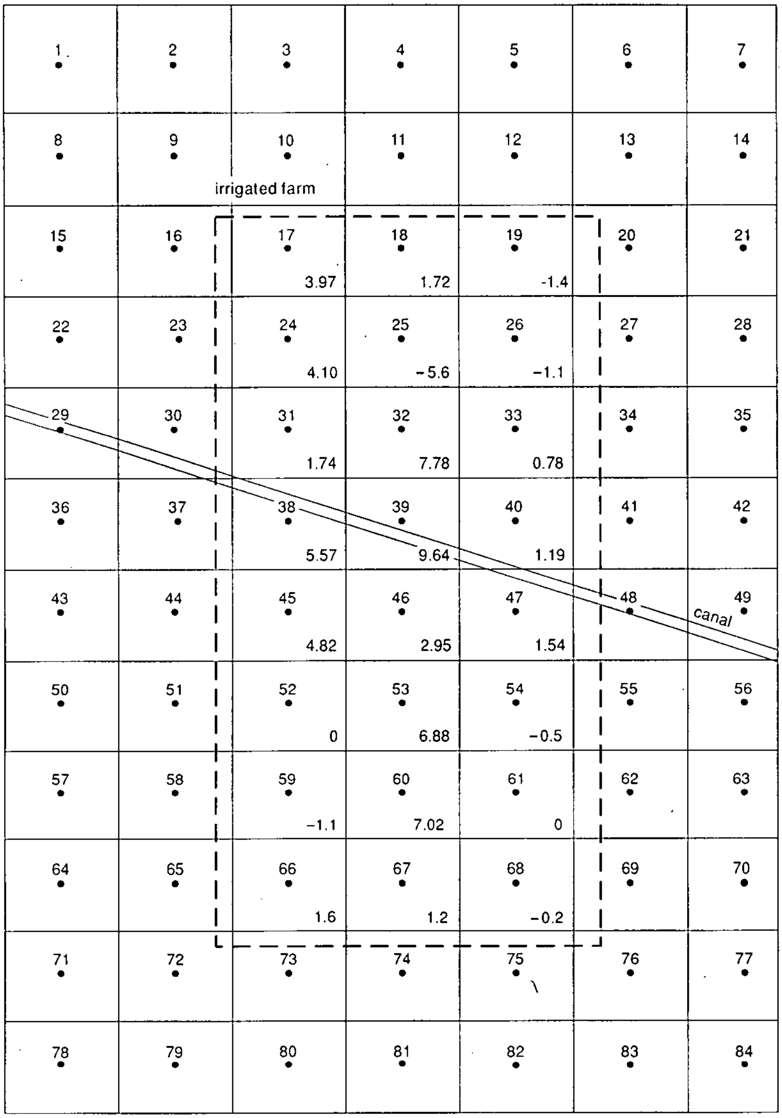


Figure 16.16 Lay-out of nodal network with nodal areas of $250 \times 200$ m$^2$ and calculated nodal net recharge values within the irrigated farm

regime that is controlled by subsurface drainage. The simulation can be done in SGMP if certain watertable levels are prescribed for each node separately. If the calculated watertable elevations exceed these levels during a simulation run, the model will introduce artificial negative flow rates. This adjustment yields calculated watertable elevations equal – within a given range – to the prescribed levels.

Two situations were simulated: one with a minimum watertable depth of 1 m and one with a minimum watertable depth of 1.5 m. Table 16.3 shows the results of the simulation runs. As expected, they showed that subsurface outflow decreases as the drainage level drops. Table 16.4 shows the drainable surplus of each nodal area in the two simulated situations with the existing watertable above the prescribed levels.

Table 16.4 shows that the actual (required) drainable surplus depends on the average watertable depth to be maintained. Table 16.4 also shows that the area in need of artificial drainage is somewhat smaller than indicated in Figure 16.12. The discrepancy means that implementing an artificial drainage system in the middle of the irrigated farm will automatically result in a greater watertable depth in the surrounding area, especially within the farm.

Note that installing a tubewell-drainage system instead of a subsurface drainage system can cause a substantial increase in the required drainable surplus if the watertable depth inside the farm drops below the levels in the area surrounding the farm; groundwater will then be 'attracted' from the surrounding areas to the farm.

By providing this kind of information, groundwater simulation models can help the drainage engineer to design subsurface drainage systems. The great advantage of these models is their ability to illustrate the consequences of man-made interference in the natural flow system without the need for actual implementation.

## 16.5 Final Remarks

Water balances can be assessed for any area and for any period. For studies of a particular area, two types of water balances can be assessed. They are:
- Water balances comprising physical entities (e.g. river catchments and groundwater basins);
- Water balances comprising only parts of physical entities (e.g. irrigation schemes and areas with shallow watertables).

The two types are very similar, their main differences being the emphasis in the first on the spatial variability of the contributing factors and the subsequent division into hydrogeological sub-areas, and the importance in the second of surface and subsurface inflow and outflow across the area's artificial boundaries. Spatial variability is less important in studies comprising relatively small areas.

Table 16.4 Drainable surplus calculated by SGMP for each nodal area (50 000 $m^2$) with watertable control (mm/d)

| Nodal area number | Watertable depth not to be exceeded | |
|---|---|---|
| | 1.0 m | 1.5 m |
| 32 | - | 2.5 |
| 39 | 5.4 | 6.6 |
| 40 | 0.5 | 3.4 |
| 45 | - | 0.5 |
| 46 | - | 0.5 |
| 47 | 4.6 | 6.7 |
| 53 | - | 1.4 |
| 54 | - | 1.9 |

Water balance studies for subsurface drainage usually fall into the second category. The need for artificial drainage often arises in areas irrigated with surface water. Irrigation is accompanied by inevitable water losses even when the efficiency (water conveyance), distribution, application, and use is relatively high (Chapter 14). The unavoidable losses from the irrigation system are usually higher than the amounts of irrigation water required for salinity control. Due to these losses, watertables in irrigated areas often rise steadily, reaching a rate of 4 m a year in exceptional situations (Schulze and De Ridder 1974). Even when this rise is slow, it will eventually lead to drainage problems. Figure 16.17 illustrates an example of such a situation. It depicts two groundwater hydrographs situated in an area where surface water irrigation started around 1900. It took some forty years before the water levels, having an initial depth of some 16 m, rose close to the land surface and then stabilized due to capillary flow and subsequent evaporation and evapotranspiration.

Groundwater recharge through infiltration and capillary rise from the shallow watertable are flow components vital to an analysis of the critical groundwater conditions and the salt balance of the rootzone. From a theoretical viewpoint, the two components do not occur simultaneously but rather over fairly long time intervals (e.g. recharge during the irrigation season and capillary rise during the subsequent fallow season). The components can appear alternately during a shorter interval (e.g. recharge while irrigation water is being applied and for 2 to 5 days afterwards, and capillary rise during the remaining days until the next irrigation).

Net groundwater inflow can be assessed from the calculation of horizontal and vertical groundwater flows. Let us consider, for example, the difference between lateral groundwater inflow and upward groundwater flow, and between lateral groundwater outflow and downward groundwater flow. Let us call this difference the 'net subsurface inflow' and give it the symbol $Q_{ni} = Q_{gi} - Q_{go}$. Clearly, net subsurface inflow can attain positive and negative values, depending on the differences in watertable elevations between the balance area and the surrounding area. The practical consequences of the value and sign of $Q_{ni}$ are important in the analysis of the groundwater regime prevailing in the balance area.

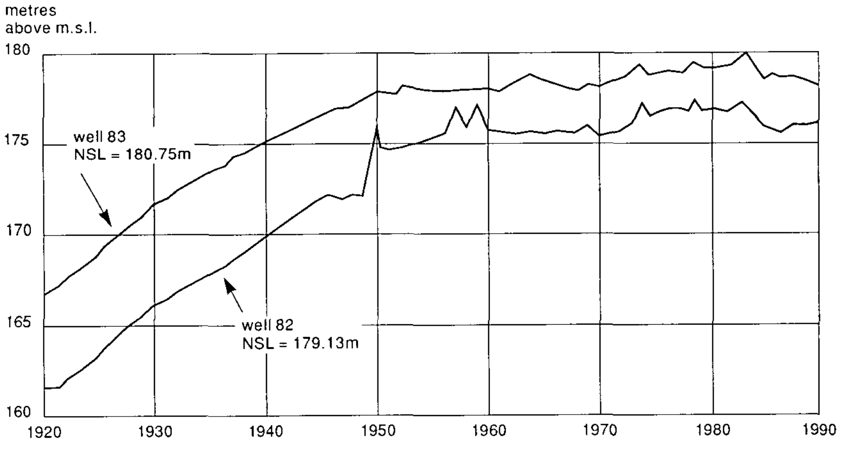


Figure 16.17 Long-term groundwater hydrographs showing rise of the watertable due to irrigation

Negative values of $Q_{ni}$ indicate that the groundwater is being recharged from the top and that there is no danger of cumulative salinization of the rootzone. But if the natural drainage cannot cope with the total recharge from percolation, the watertable will rise to unacceptable heights or remain at already shallow depths, and subsurface drainage will still be necessary to control it.

Positive values of $Q_{ni}$ indicate that groundwater is 'lost'. Under natural conditions this situation often occurs in topographical depressions and low-lying valley bottoms. In these areas, the shallow groundwater system loses part of its water to capillary rise and subsequent evapotranspiration. Artificial drainage is then required to control the watertable and protect the rootzone against cumulative salinization. Positive values of $Q_{ni}$ also occur in areas where groundwater is abstracted by tubewells for drinking water and irrigation. Artificial drainage is usually not required under these conditions.

## References


Boonstra, J. and N.A. de Ridder 1990. Numerical modelling of groundwater basins, 2nd. ed. ILRI Publication 29, Wageningen, 226 p.

Brown, R.H., A.A. Konoplyantsev, J. Ineson and V.S. Kovalevsky 1977. Groundwater studies – an international guide for research and practice. Studies and reports in hydrology, vol. 7. Unesco, Paris.

Colenbrander, H.J. 1970. Hydrologisch onderzoek in het Leerinkbeek gebied : 2e interim rapport. Provincie Gelderland, Arnhem, 335 p.

Dalton, J. 1802. Experiments and observations to determine whether the quantity of rainfall and dew is equal to the quantity of water carried off by the rivers and raised by evaporation, with an enquiry into the origin of springs. Mem. Proc. Lit. Phil. Soc., Manchester 5, part 2, pp. 346-372.

Dooge, J.C.I. 1984. The water of the earth. Hydrol. Sci. J., 29, 2, 6, pp. 149-176.

Doorenbos, J. and W.O. Pruitt 1977. Crop water requirements. FAO Irrigation and Drainage Paper 24, Rome, 144 p.

Feddes, R.A., P. Kabat, P.J.T. van Bakel, J.J.B. Bronswijk and J. Halbertsma 1988. Modelling soil water dynamics in the unsaturated zone – state of the art. J. Hydrol., 100, pp. 69-111.

IGWMC 1992. IGWMC Software Catalog. Golden, Colorado, 40 p.

Lohman, S.W. 1972. Groundwater hydraulics. I.S. Geological Survey, Professional Paper 708. U.S. Government Printing Office, Washington, 70 p.

Schulze, F.E. and N.A. de Ridder 1974. The rising watertable in the West Nubarya area of Egypt. Nature and Resources 10, 1, pp. 12-18.

Volp, C. and A.C.W. Lambrechts 1988. The SAMWAT database for computer models in water management. SAMWAT Report, 2, The Hague, 142 p.